| REPORT DOCUMENTATION PAGE | | Form Approved OMB No. 0704-0188 |
|---|---|---|

Public reporting burden for this collection of information is estimated to average 1 hour per response, including the time for reviewing instructions, searching existing data sources, gathering and maintaining the data needed, and completing and reviewing the collection of information. Send comments regarding this burden estimate or any other aspect of this collection of information, including suggestions for reducing the burden, to Department of Defense, Washington Headquarters Services, Directorate for Information Operations and Reports (0704-0188), 1215 Jefferson Davis Highway, Suite 1204, Arlington, VA 22202-4302. Respondents should be aware that notwithstanding any other provision of law, no person shall be subject to any penalty for failing to comply with a collection of information if it does not display a currently valid OMB control number.
**PLEASE DO NOT RETURN YOUR FORM TO THE ABOVE ADDRESS.**

| 1. REPORT DATE *(DD-MM-YYYY)* | 2. REPORT TYPE | 3. DATES COVERED *(From – To)* |
|---|---|---|
| 31-03-2010 | Final Report | 1 January 2006 - 01-Jan-07 |

**4. TITLE AND SUBTITLE**

Bio Organic-Semiconductor Field-Effect Transistor (BioFET) Based on Deoxyribonucleic Acid (DNA) Gate Dielectric

**5a. CONTRACT NUMBER**
FA8655-07-1-3026

**5b. GRANT NUMBER**

**5c. PROGRAM ELEMENT NUMBER**

**6. AUTHOR(S)**

Professor Niyazi Serdar Sariciftci

**5d. PROJECT NUMBER**

**5d. TASK NUMBER**

**5e. WORK UNIT NUMBER**

**7. PERFORMING ORGANIZATION NAME(S) AND ADDRESS(ES)**
Johannes Kepler University of Linz
Altenbergerstr. 69
Linz A-4040
Austria

**8. PERFORMING ORGANIZATION REPORT NUMBER**

N/A

**9. SPONSORING/MONITORING AGENCY NAME(S) AND ADDRESS(ES)**

EOARD
Unit 4515 BOX 14
APO AE 09421

**10. SPONSOR/MONITOR'S ACRONYM(S)**

**11. SPONSOR/MONITOR'S REPORT NUMBER(S)**
Grant 07-3026

**12. DISTRIBUTION/AVAILABILITY STATEMENT**

Approved for public release; distribution is unlimited.

**13. SUPPLEMENTARY NOTES**

**14. ABSTRACT**

A nonvolatile memory device has a structure of a metal oxide semiconductor field effect transistor (MOSFET) where the conventional gate electrode is modified in a way to enable temporary charge storage inside the gate. The time when the stored charge decreases to 50% of its initial value is defined as retention time. A long retention time is required for nonvolatile memory devices. Using inorganic semiconductors like Si, this has been used in integrated circuits since the last four decades. Typically there are two types of nonvolatile memory devices, floating gate devices and metal-insulator-oxide-semiconductor (MIOS) devices. First attempts to use polarizable gate insulators in combination with organic semiconductors. The field effect transistors showed floating gate effects, but the potential for organic memories was not realized. Recently insulators based on polymeric ferroelectric-like materials were utilised to fabricate nonvolatile organic memory devices [18-21].

One of the disadvantages of use of such polymeric ferroelectric-like materials is the very high surface roughness which does not allow forming smooth interface between insulator and organic semiconductor. As a result, on and off ratio and on current becomes extremely critical issue. We have demonstrated successfully a combination of a polymer space charge electret and an organic semiconductor in a field effect transistor configuration. Our initial experiments concerns with the study of the thin film morphology. Figure 5(a) shows the morphology of a 200 nm DNA-CTMA film spun on quartz substrate which resulted a surafe roughness of 10 nm. Features of self organised structures are observed. Fig. 5(b) shows the dielectric response (C-V) of the sandwiched DNA-CTMA film between the two electrodes (MIM) devices. It appears that DNA-CTMA film shows stable capacitance, C for a wide range of frequency with absolute capacitance of ~1.15 nF/cm2. From the measurement of capacitance per unit area we obtained a dielectric constant of $\mathit{\acute{O}}$ DNA = 7.8.

**15. SUBJECT TERMS**
EOARD, Electronic Devices, Electronics and Electrical Engineering, Biomaterials

| 16. SECURITY CLASSIFICATION OF: | | | 17. LIMITATION OF ABSTRACT | 18, NUMBER OF PAGES | 19a. NAME OF RESPONSIBLE PERSON |
|---|---|---|---|---|---|
| **a. REPORT**<br>UNCLAS | **b. ABSTRACT**<br>UNCLAS | **c. THIS PAGE**<br>UNCLAS | UL | 30 | A. GAVRIELIDES |
| | | | | | **19b. TELEPHONE NUMBER** *(Include area code)*<br>+44 (0)1895 616205 |

**Standard Form 298** (Rev. 8/98)
Prescribed by ANSI Std. Z39-18

# DNA Based Bio-Organic Field-Effect Transistors

## FINAL REPORT FOR JANUARY 2007-SEPTEMBER 2009

For the Cooperative Grant Agreement with

## EUROPEAN OFFICE OF AEROSPACE RESEARCH AND DEVELOPMENT

Award Number: FA 8655-07-1-3026

Reported by *Linzer Institut für Organische Solarzellen (LIOS)*

Author:

*o. Univ.-Prof. Dr. Niyazi Serdar Sariciftci*

Experimental studies done by:

*Philipp Stadler and Dr. Birendra Singh*

Linz, Oktober 2009

## Executive Summary

Biomolecular DNA, as a marine waste product from salmon processing has been exploited as biodegradable polymeric material for photonics and electronics. For preparing high optical quality thin films of DNA, a method using DNA with cationic surfactants such as DNA-cetyltrimethylammonium, CTMA has been developed by the group of Dr. James Grote, US Air Force Labs. This is the starting basis of a fruitful collaboration between US Air Force Labs (group of Dr. James Grote) and Linz Institute for Organic Solar Cells (LIOS) at the Johannes Kepler University in Linz, Austria (Prof. Sariciftci).

This process using CTMA enhances solubility and processing of DNA for thin film device fabrication. It revealed that this DNA-CTMA complexes were thermostable up to 230 °C with a high transparency from 300 to about 1000 nm. Due to its nature of large band gap and large dielectric constant, thin films of DNA-CTMA has been successfully used in multiple applications such as organic light emitting diodes (OLED), a cladding and host material in nonlinear optical devices, and organic field-effect transistors (OFET). Using this DNA based biopolymers as a gate dielectric layer, OFET devices were fabricated that exhibits current-voltage characteristics with low voltages as compared with using other polymer-based dielectrics. Using a thin film of DNA-CTMA based biopolymer as the gate insulator and pentacene as the organic semiconductor, we have demonstrated a bio organic FET or BioFET in which the current was modulated over three orders of magnitude using gate voltages less than 10V. Given the possiblity to functionalize the DNA film customized for specific purposes viz. biosensing, DNA-CTMA with its unique structural, optical and electronic properties results in many applications that are extremely interesting.

During the three years of collaboration between LIOS and US Air Force Labs. We have had visitors (Dr. James Grote and Dr. Joshua Hagen) from USA in Linz. Our results have been published in several high ranked international scientific journals. This fact clearly and objectively demonstrates the scientific quality and success of this collaboration project.

•Th. B. Singh, N.S. Sariciftci, J. Grote, F. Hopkins,

*Journal of Applied Physics* **100** (2006), 024514.

• P. Stadler, K. Oppelt, B. Singh, J. Grote, R. Schwödiauer, S. Bauer, H. Piglmayer-Brezina, D. Bäuerle, N.S. Sariciftci, *Organic Electronics* **8** (2007), 648-654.

•P. Stadler, *Master thesis, Linz Institute of Organic Solar Cells (LIOS), Johannes Kepler University of Linz, Austria,* 2007

•C. Yumusak, B. Singh, N.S. Sariciftci, G. Grote
*Applied Physics Letters* **95** (2009), 263304

•T. B. Singh, N. S. Sariciftci, J. G. Grote
*Advanced Polymer Science* **223** (2010), 189-212

**Abbreviations used in this report:**

*LCD: liquid crystal displays*

*CTMA: hexadecyltrimethylammmonium chloride*

*EBL: electron blocking layer*

*PEDOT : [poly(3,4-ethylenedioxythiophene)]*

*PSS: poly(4-styrenesulfonate)*

*NPB: (N,N'-bis(naphthalene-1-yl)-N,N'-bis(phenyl)benzidine)*

*$Alq_3$ : tris-(8-hydroxyquinoline) aluminum*

*BCP: 2,9-dimethyl-4,7-diphenyl-1,10-phenanthroline*

*HBL: hole blocking layer*

*ETL: electron transport layer*

*EIL : electron injection layer*

*BioLED: bio organic light emitting diodes*

*BioFET: bio organic field-effect transistors*

*PCBM: 1-(3-methoxycarbonyl)propyl-1-phenyl [6,6]$C_{61}$*

$V_t$ : *threshold voltage*

$V_{Drain}$: *drain voltage*

$V_{Gate}$ : *gate voltage*

$I_{Drain,Sat}$ : *saturated drain current*

*T:temperature*

# 1. Introduction

The progress made in the field of organic electronics in the last two decades have resulted in the demonstration of prototype devices such as 4.7-inch QVGA active matrix display containing 76,800 organic transistors [1], mechanical sensors[2] and chemical sensors [3]. Devices such as organic light emitting diodes (OLEDs), which is a vital part of display technology is now used in consumer electronics in place of LCD (See www.sony.com). All these have been possible with the availability of a variety of organic materials, conducting polymers., insulators, semiconductors and metals. Apart from conventional organic materials, biomaterials are of particular interest. Biomaterials show often unusual properties which are not easily replicated in conventional organic or inorganic materials. In addition to this, natural biomaterials are from renewable resources and are inherently biodegradable. Among natural biodegradable materials, the science community has shown interest to DNA for various reasons such as potential use of DNA assembly in molecular electronic devices[4], nanoscale robotics[5] and DNA-based computation[6].

The molecular structure of DNA (double helix) consists of two inter-twined spirals of sugar and phosphate molecules linked by hydrogen-bonded base pairs (See Figure 1).
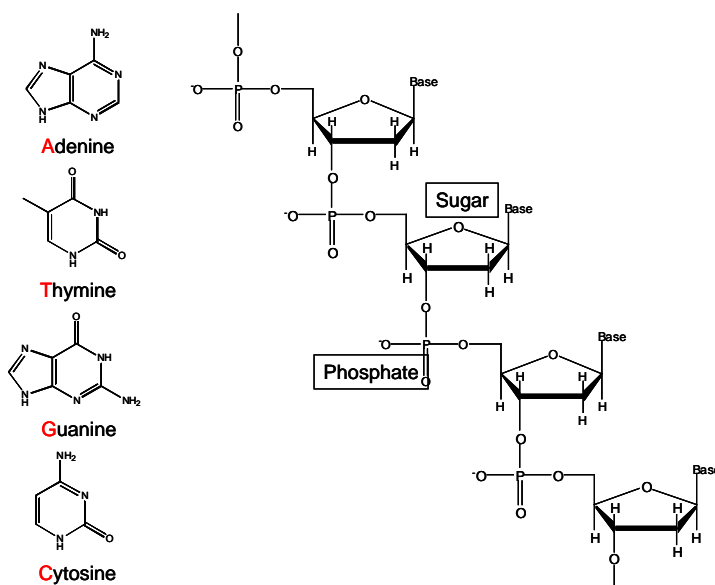


Figure 1: Phosphate-sugar backbone of single strand DNA.

The phosphate backbone is negatively charged with H+ or Na+ to balance the neutrality. The width of the double helix is about two nanometres and the length of the DNA molecule depends on the number of base pairs (about a third of a nanometre per base pair). For practical use,  natural DNA fish waste, for example salmon sperm, which is normally a waste product of the salmon-fishing industry is attractive (See Figure 2-3). Although there is a wealth of knowledge on nature of transport properties on synthetic DNA, in this project we have focussed only on DNA materials derived from salmon milt. Reader may also pay attention that there is an ongoing dabate on insulating [7-12], semiconducting [13-14] as well as highly conducting [15] and even superconducting nature [16] of transport in DNA molecules.



meat and roe are edible

milt & roe sacs as a waste product

Figure 2:      Illustration of salmon as an edible meat and as a source of natural biomaterials (salmon DNA).

## 2. DNA-CTMA as Optoelectronic Material

The DNA used for research in optoelectronic devices was purified DNA provided by the Chitose Institute of Science and Technology (CIST) [17-18]. The processing steps involved are summarised in Figure 2 and 3. The starting point was marine-based DNA, first isolated from frozen salmon milt and roe sacs through a homogenization process. It then went through an enzymatic treatment to degrade the proteins by protease. Resulting freeze dried purified DNA has

molecular weight ranging from 500,000-8,000,000 Da with purity as high as 96% and protein content of 1-2%.
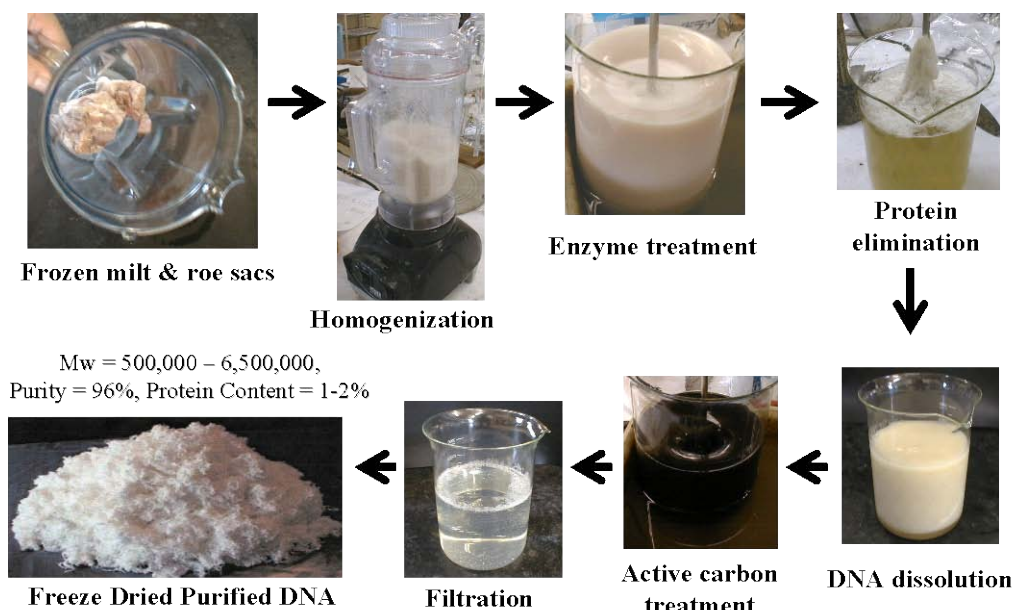


Figure 3: Illustration of purifying steps of salmon DNA from its frozen milt and roe sacs

The average molecular weight of DNA provided by CIST is on average, greater than 8,000,000 Da. If necessary, the molecular weight of DNA supplied by CIST can be tailored and cut using an ultrasonic procedure [24] which gives rise to lower molecular weight of 200,000 Da depending the sonication energy as shown in Figure 4.
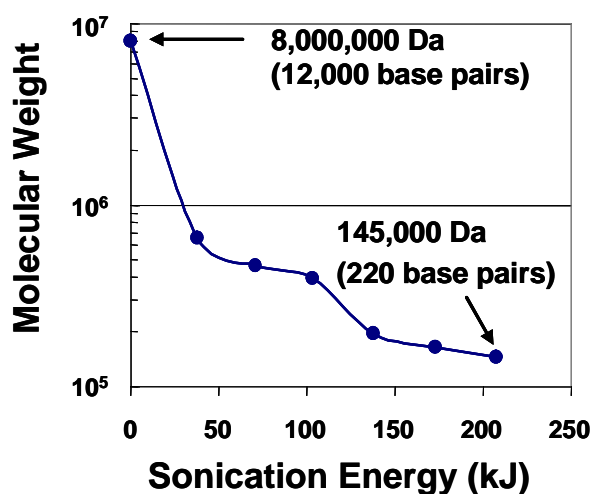


Figure 4: Molecular weight of DNA as a function of total sonication energy.

The DNA was sonicated on ice in 10 s long pulses with a 20 s rest period between pulses to prevent overheating of the sample.

It was found that the purified DNA was soluble only in water, the resulting films are too water sensitive and have insufficient mechanical strength, so not compatible with typically fabrication processes used for polymer based devices. It has also been observed that many particulates are present in the DNA films. Therefore, additional processing steps are performed to render DNA more suitable for device fabrication with better film quality. From the knowledge of stoichiometric combination of an anionic polylectrolyte with a cationic surfactant, it has been shown that DNA which is an anionic polyelectrolyte could be quantitatively precipitated with cationic surfactant in water [19]. This processing was accomplished by precipitating the purified DNA in water with a cationic surfactant complex, hexadecyltrimethylammmonium chloride (CTMA), by an ion exchange reaction [20-25] [See Figure 5].
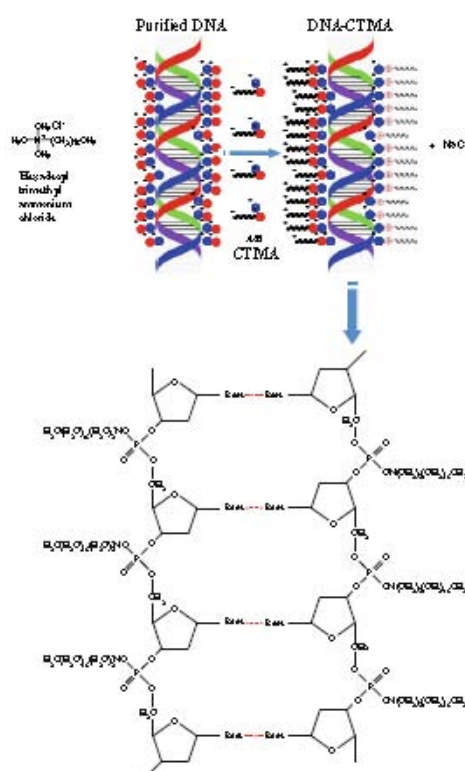


Figure 5:    DNA-CTMA is formed by adding surfactant groups of CTMA to the back bone of DNA. Chemical structure of CTMA: Hexadecyl Trimethyl-ammonium Chloride or Cetyltrimethylammonium chloride is also shown. The 2-D schematic diagram shows how surfactants are added to the DNA structure.

This surfactant was selected for the following reasons [17]: Cationic surfactants having longer (>16) alkyl chains are water-insoluble, and chains shorter than $C_{16}$ might induce poor mechanical property of the materials. Second, DNA complexes made with longer alkyl chains might damage the double helix structure of DNA as the strong association and aggregation among alkyl chains might break the hydrogen bonds of the nucleobase pairs. The third reason is that these surfactants are commercially available. The resulting DNA-lipid complex became water insoluble and more mechanically stable due to the alkyl chain of the CTMA. Adding the CTMA complex, DNA-CTMA could now be dissolved using solvents more compatible with device fabrication, such as chloroform, ethanol, methanol, butanol or a chloroform/alcohol blends. When dissolved in the organic solvent the DNA-CTMA was passed through a 0.2 μm filter to remove any large particulates.

DNA-CTMA films can be cast by standard methods like spin coating, doctor blading, dip coating drop casting etc and exhibit excellent transmission over a broad wavelength range.
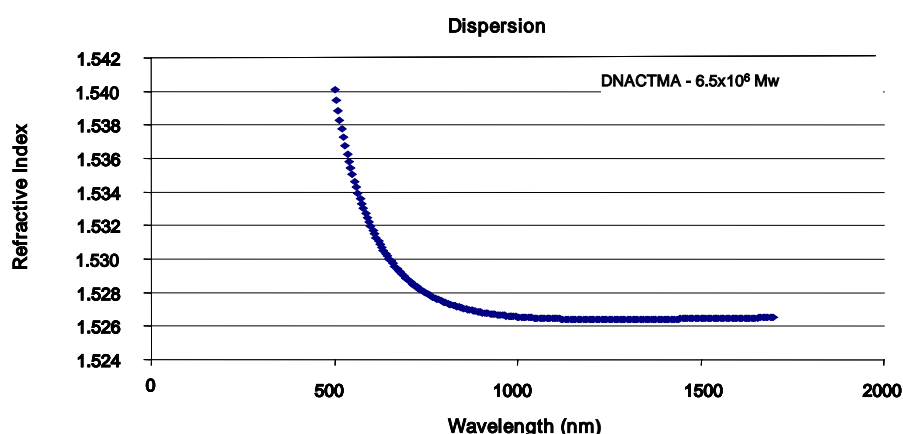


Figure 6:     Refractive index of DNA-CTMA.

DNA-CTMA is also a very low loss optical material applicable over a broad range of wavelengths with refractive index ranging from 1.526 to 1.540 (see Figure 6). The electrical resistivity of DNA-CTMA films with molecular weights of 500,000 and 6,500000 as a function of temperature are in the range of $10^9$-$10^{14}$ Ω-cm depending on the molecular weight (See Figure 7). Dielectric constant of DNA-CTMA is 7.8-6 at the frequency range of 1-1000 KHz (See Figure 8). Thermo-gravimetric analysis (TGA) of the DNA-CTMA complex shows stability up to 230 °C and 10% water absorption in air at room temperature (See Figure 9).
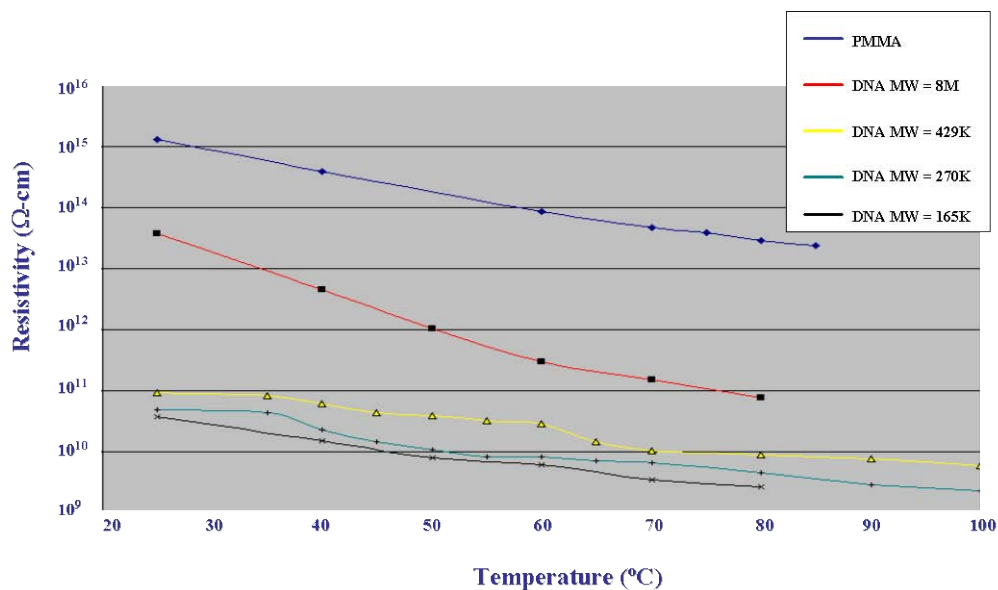
Figure 7:     Resistivity vs. temperature for DNA-CTMA complexes with varying molecular weight and PMMA as a reference.
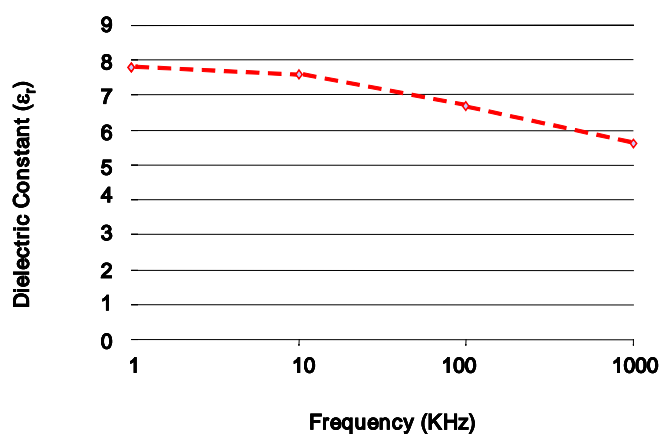


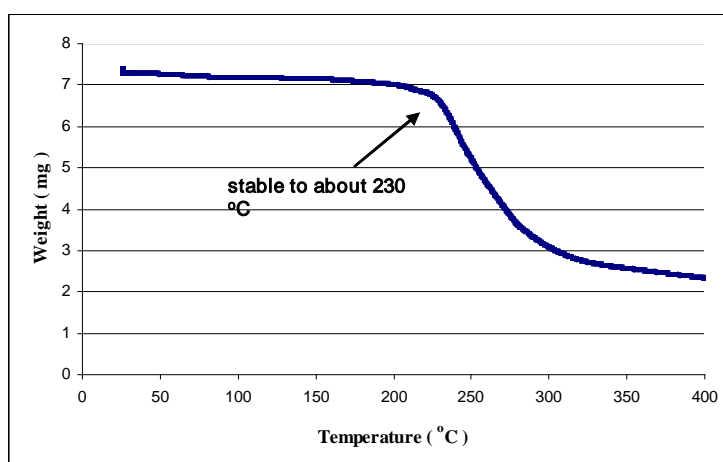Figure 8:     Dielectric constant versus frequency for DNA-CTMA complex.



Figure 9:     Thermo-galvometric analysis (TGA) of DNA-CTMA material.

# 3. DNA-CTMA in organic field effect transistors (BiOFETs)

DNA-CTMA films have been successfully used as gate dielectric in OFETs. OFETs have been fabricated with various device geometries as depicted in Fig. 10.
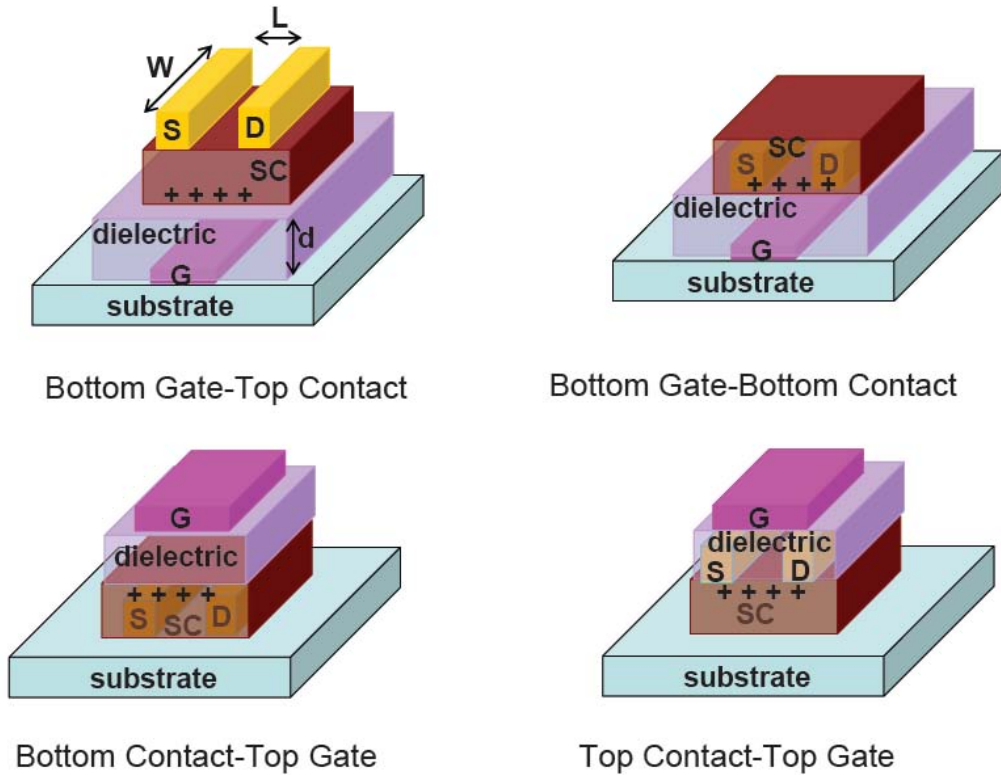


**Figure 10:** Schematic of the bottom-gate organic field-effect transistors (OFETs) with (a) top contact (b) bottom contact structures. Schematic diagram of a (c) top-gate/bottom contact OFETs using a standard TFT device structures and (d) top-gate /top contact is also shown.

The most commonly used device geometry are bottom gate with top contact and bottom gate with bottom contact partly because of borrowing the concept of thin-film silicon transistor (TFT) using thermally grown $Si/SiO_2$ oxide as gate dielectric as subtrate. Due to the advantage of having commercially available high quality $Si/SiO_2$ substrate, it has dominated the whole community in the last decades. Recently, selected organic dielectrics (See Figure 11) are also successfully employed for high performance OFETs [28-37]. Organic dielectrics

(i) can be solution-processed,

(ii)     provide smooth films on transparent glass and plastic substrates,

(iii)     are suitable for opto-electronics like photo-responsive OFETs due to their high optical transparency,

(iv)     can be thermally stable up to 200 $^0$C with a relatively small thermal expansion coefficient, and
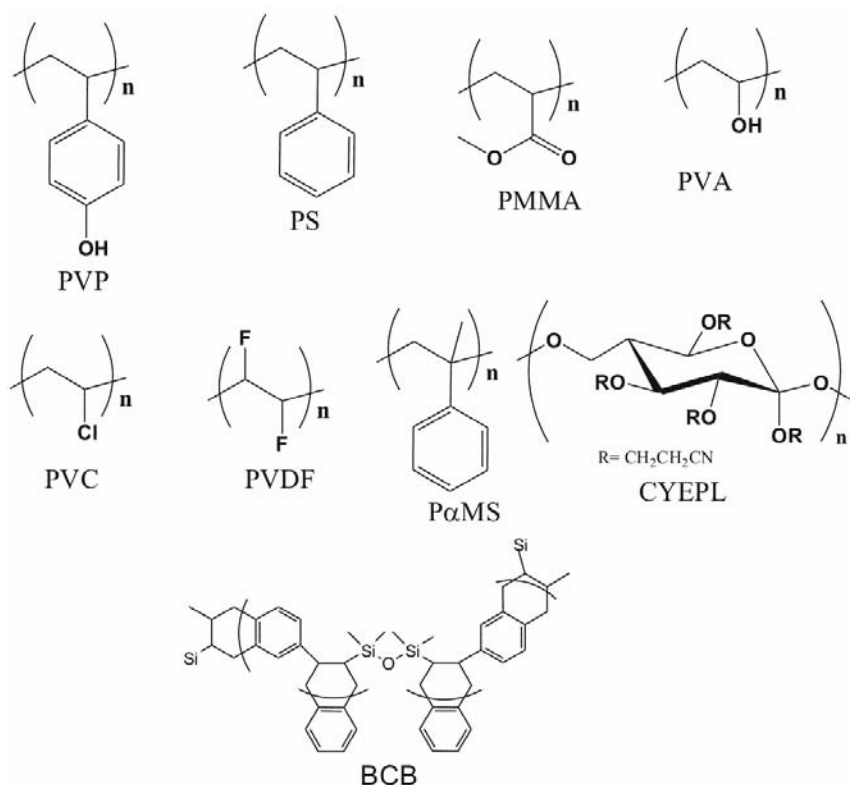


Figure 11:     Chemical structure of some commonly used organic dielectric. PVP: Poly(4-vinyl phenol); PS: Polystyrene; PMMA: polymethyl-methacrylate ; PVA: polyvinyl alcohol; PVC: polyvinylchloride; PVDF: polyvinylidenfluoride; PαMS: poly[α-methylstyrene], CYEPL: cyano-ethylpullulan and BCB: divinyltetramethyldisiloxane-bis(benzocyclobutene).

It was very recently demonstrated that thin films of DNA-CTMA can be employed as a dielectric for low voltage operating OFETs [38]. This stems from the fact that thin films of DNA-CTMA are relatively smooth depending on the molecular weight as shown with atomic force microscope AFM in Figure [12(a-b)]. A smooth film of dielectric layer is a prerequisite to enable deposition of smooth organic semiconductor forming a better interface for charge transport.
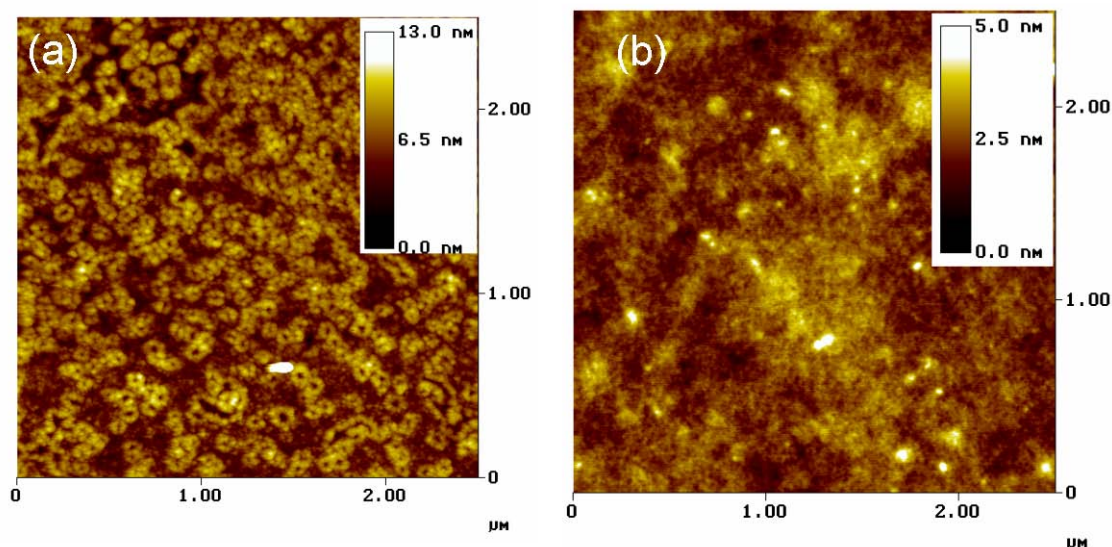
11

Figure 12:    AFM topographical images (2.5 µm x 2.5 µm) of spin-coated film of (a) 200 nm film of 8M mol.wt. DNA-CTMA and (b) 1 µm thick film of 300 kDa molecular wt. DNA-CTMA.

Another important property is the large capacitive coupling enabled due to relatively large dielectric constant of 7.8 for DNA-CTMA. A study on the thin film morphology of DNA-CTMA reveals formation of self-organised structures in DNA-CTMA thin-films with higher molecular of 8M mol. wt. These self-assembled DNA-surfactant complex materials, with good processability will have promising applications in molecular optoelectronic fields. It was proposed that such a self-organised structure arises because the alkyl chains are oriented perpendicular to film plane, and chiral DNA helices were oriented in the direction parallel to the film plane [17].

In an effort to demonstrate, low voltage operating BioFETs, two organic semiconductors pentacene and 1-(3-methoxycarbonyl) propyl-1-phenyl [6, 6]$C_{61}$ (PCBM) were employed as an active semiconductor. Both are well known in the field as a benchmark high mobility p-type and n-type semiconductors respectively. Structure of fabricated OFETs are depicted in Fig. 13.
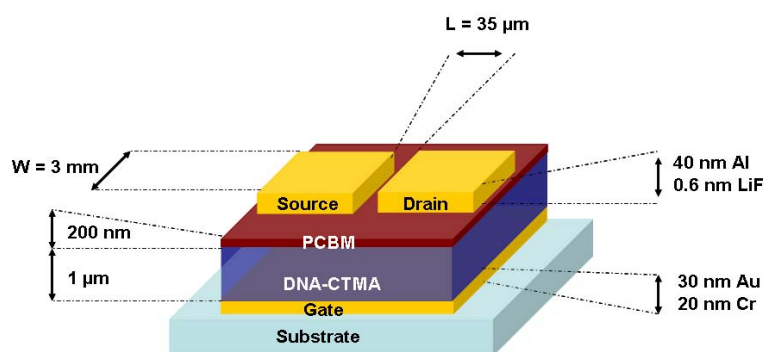
Figure13: Top-contact/bottom-gate OFET structure including geometric device parameters

Energy level diagrams of respective materials used for p-channel as well an n-channel BioFTEs are depicted in Figure 14. Various devices such as Metal-insulator-Metal (MIM) and Metal-insulator-Semiconductor (MIS) devices were also fabricated using DNA-CTMA as an insulator and PCBM as semiconductor.
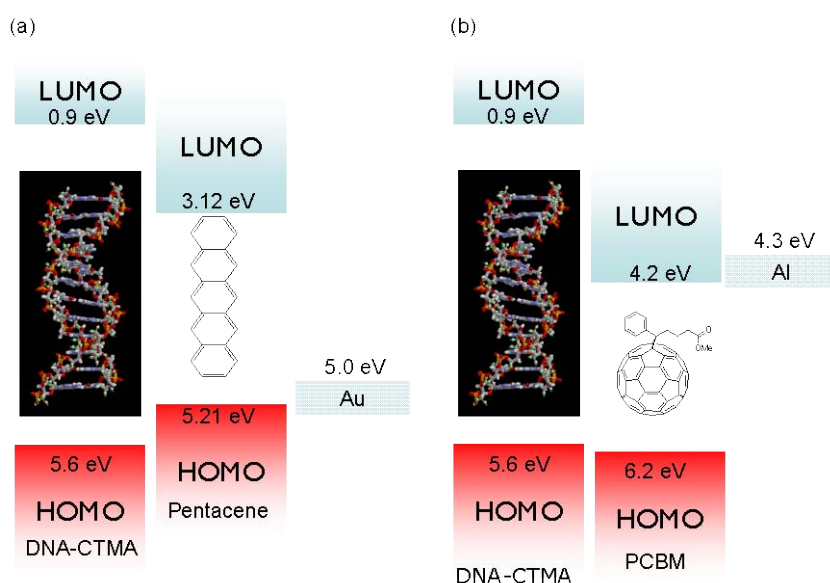


Figure 14:    Energy level diagram without taking into account of interface dipole layers of the respective materials for use in fabrication of (a) p-type BioFET with pentacene as a semiconductor and using Au as source-drain contact (b) for a n-type BioFET with PCBM as a semiconductor and using Al and source-drain contact.

Surface morphology studies of as deposited organic semiconductor film on top of a DNA indicate a surface roughness of 80 nm for room temperature evaporated pentacene film with an average pentacene crystallites ca. 200 nm is observed (see Figure 15(a)) whereas a surface roughness of about 2 nm for solution deposited PCBM on top of DNA. For comparison, larger crystallites of pentacene are usually obtained when using more common organic dielectrics as bottom gate layer. Higher smoothness of PCBM thin film can be attributed to its highly soluble nature.
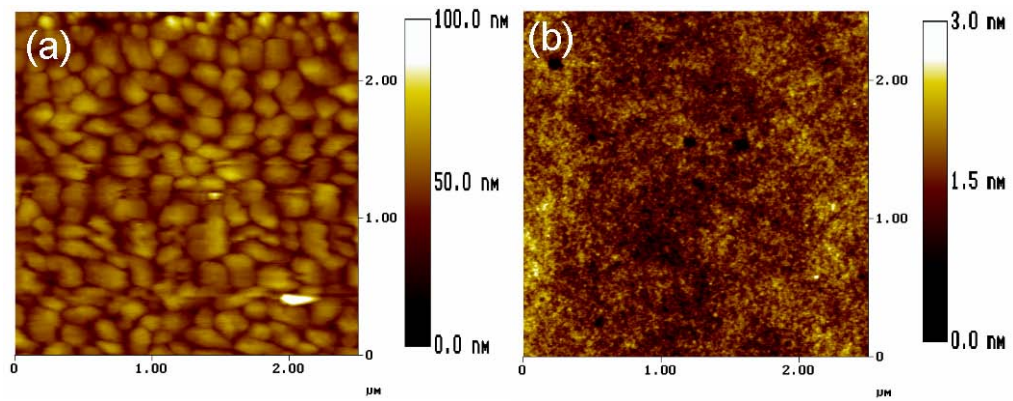


Figure 15:       (a) AFM topographical images (2.5 µm x 2.5 µm) of 50 nm film of pentacene evaporated on DNA-CTMA. (b) AFM topographical images (2.5 µm x 2.5 µm) of 100 nm spin-coated film of PCBM on DNA-CTMA,

The scheme of p-channel BioFET device scheme is shown in Figure 16(a). Typical output characteristics of the p-channel BioFET is shown in Figure 16(b). With 200 nm thick film of DNA-CTMA dielectric layer and a 50 nm thin film of pentacene semiconductor, the saturated drain current, $I_{Drain,Sat}$ was able to modulate over three orders of magnitude using gate voltages less than 10 V. Figure 16(c) is a plot of the transfer characteristics for p-channel BioFET. Pronounced hysteresis in the transfer characteristics can be observed in these devices, as indicated by the direction of arrows. Similarly, n-channel BioFET characteristic are shown in Figure 17. Figure 17(a) shows the output characteristics of n-channel BioFETs with PCBM as a semiconductor with LiF/Al source-drain electrodes. Since LiF/Al was employed as source drain electrode, which are favourable for electron-injection, a p-channel BioFET with PCBM as a

semiconductor is not expected due to large hole injection barrier [$\phi_b(h^+) = 1.2$ eV] from these electrodes into PCBM [39].
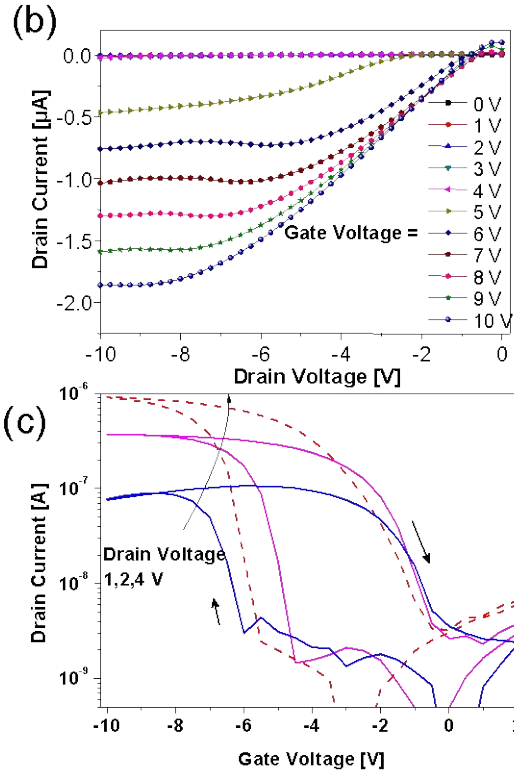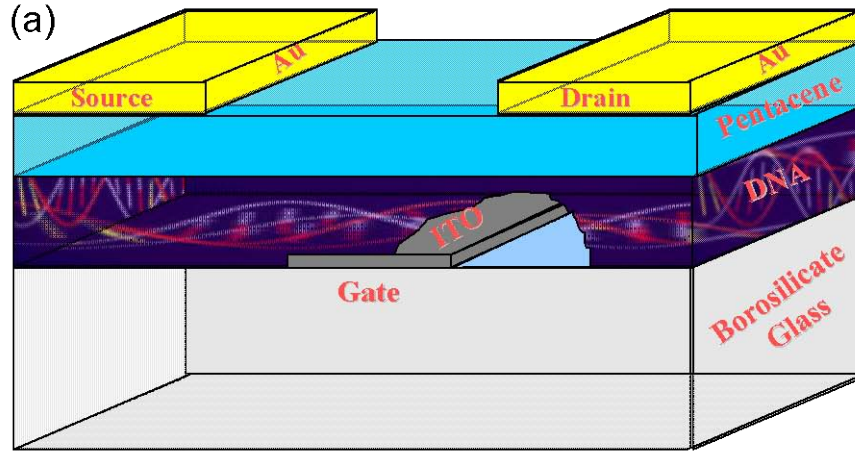


Figure 16:    (a) Schematic of the top contact BioFET device employing pentacene as a semiconductor and 8 M mol wt DNA-CTMA as a dielectric. (b) Corresponding BioFET output characteristics; drain current, $I_{ds}$ vs. versus drain voltage, $V_{ds}$ for different gate voltages, $V_{gs}$ (c) Transfer characteristics; $I_{ds}$ vs $V_{gs}$ for drain voltages, $V_{ds} = 1$, 2 and 4 V.
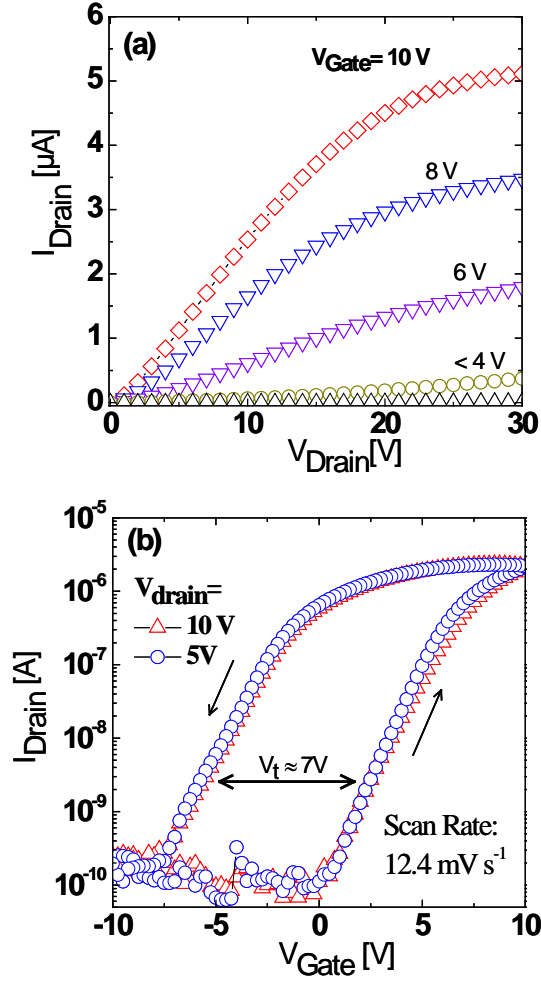
Figure 17: (a) Output characteristics of solution-processed low voltage operating n-channel BioFET with voltage step of 1 V/Sec. (b) Transfer characteristics of BioFET. All measurements are performed with steps of 12.4mVs$^{-1}$. Note: gate current characteristics of the BioFET, also plotted, correspond to the right scale of the graph.

As can be seen in Figure 17(a), $I_{Drain,Sat}$ can be as high as 4-5 µA, for a device with channel length of 35 µm and width of 3 mm and for $V_{Drain} = 20$ V and $V_{Gate} \approx$ 10 V. This is promising when compared to standard organic dielectric based PCBM OFETs with an operating voltage in the range of > 60 V at the same geometry [37]. The lower operating voltage of the n-channel BioFET is even clearer from its transfer characteristics as shown in Figure 17(b). The threshold voltage, $V_{th}$, is found to be different from standard PCBM OFETs using other

organic gate dielectrics, even though the thickness of the dielectrics and other device parameters are similar [39]. A lower $V_{th}$ observed is an indication of excellent dielectric coupling between DNA-CTMA and PCBM. Forward and reverse scan with scan rate of 12.4 mVs$^{-1}$ give rise to hysteresis with shift in $V_{th}$ by 7V.

Possible reasons for observation of hysteresis in OFETs have been investigated extensively in the past couple of years. They are mainly attributed to the
(i) charge trapping and release in the bulk of the semiconductor
(ii) Due to the polarizable gate dielectric
(iii) dipole polarization and
(iv) electret effect due to mobile ions in the dielectric

## 4 Dielectric spectroscopy of DNA-CTMA thin films

Studies of capacitance-voltage characteristics were done on metal insulator semiconductor (MIS) structures. The MIS structure consists of PCBM spin-coated on top of DNA-CTMA. For the metal electrode in the MIS device we have chosen Cr/Au was chosen as a bottom as well as top electrodes. Similarly MIM devices were also fabricated and studied. For the MIM devices characteristics of capacitance vs. frequency shows no significant change in capacitance throughout the measured frequency range (see Figure 18). On the other hand, MIS devices shows rise in capacitance of between frequency ranges of $10^1$ to $10^{-2}$ Hz corresponding to the dielectric relaxation of the PCBM semiconductor. At lower frequency, capacitance further increases to an unrealistic capacitance considering the series capacitance of DNA-CTMA and PCBM layer. This sharp rise in capacitance can be attributed due to trap charges or impurities such as ions which is most likely in the bulk of DNA-CTMA as well as at the interface.. Studies of dielectric loss (tan δ) reveal more vital information about DNA-CTMA as a rather lossy dielectric as shown in Figure 18(b). A strong increase of tan δ values on the order of 1 for MIM and 100 for MIS at low frequencies can be an indication of Maxwell-Wagner effect [41].

Studies of capacitance vs. electric field at different sweeping rate were also carried out for MIS devices (see Figure 18(c)). As evident from the Figure18(c), the slower the scan rate, the larger is the hysteresis.
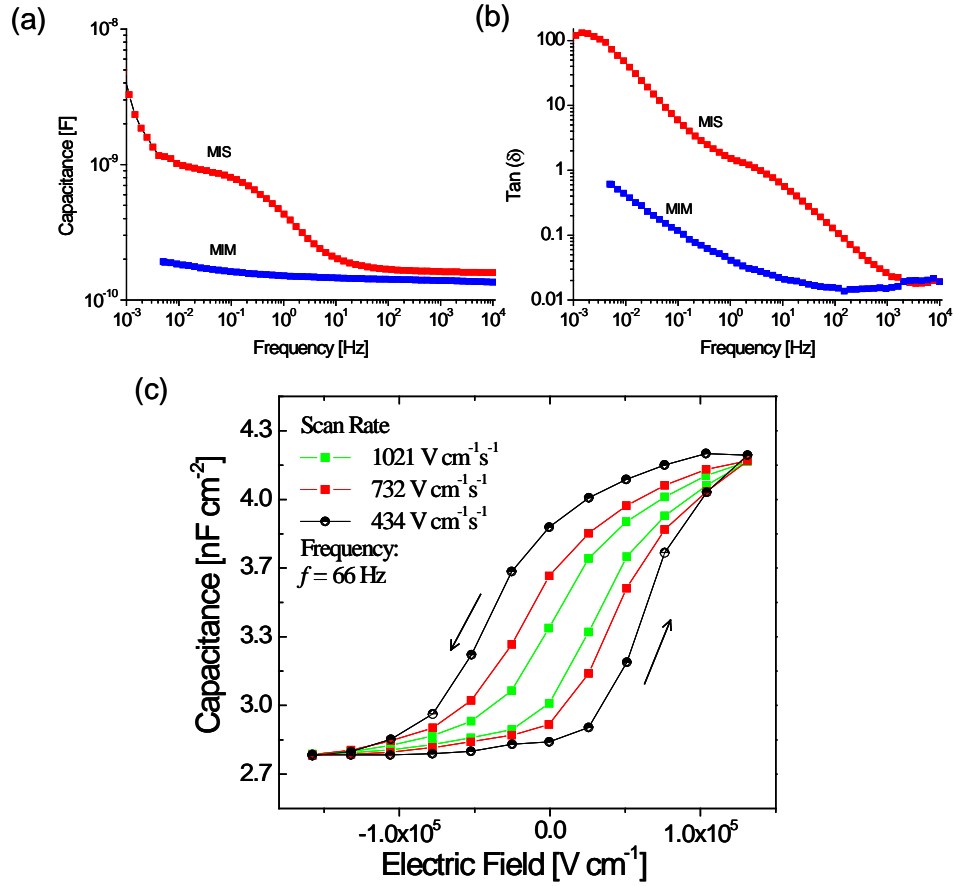


Figure 18: Room-temperature capacitance-frequency characteristics (a) MIM and MIS structure devices (with applied a.c. voltage of 0.5 V), (b) Tan ($\delta$)-frequency characteristics and (c) Quasi-static capacitance-electric field curves for the MIS structures in (at 66 Hz) at different sweep/scan rate ($dV_{\text{Gate}}/dt$) as indicated. Larger hysteresis with slower scan rates are found.

Further, from the studies of the real part of impedance[40], Z´ and imaginary part of Z´´ of the MIS devices, it was found out that a simple model based on series connection of two capacitors and resistors for the two layers cannot explain the observed phenomena [see Figure 19]. It gives an impression that interfacial layer formation between the DNA-CTMA and PCBM layer can be crucial. This observation raises question whether DNA-CTMA possesses the properties of non-linear charge polarization effect. The nature of polarization can be obtained from

the quasi-static measurement on MIM devices. As shown in Figure 20, the shape of the current-voltage characteristics for a slowly varying ramp voltage is quasi-linear which indicated that DNA-CTMA have quasi-linear polarization effect. Furthermore a plot of surface charge density vs. applied voltage shows that all the curves passed through the origin which rules out possibility for nonlinear charge polarization.
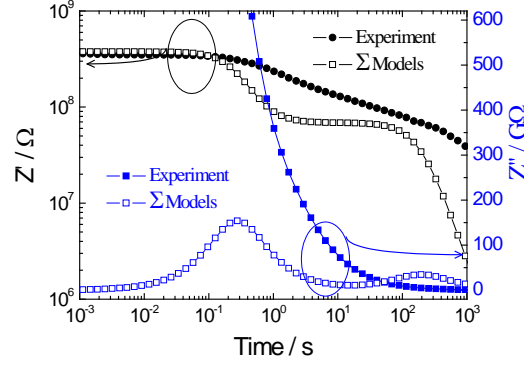


Figure 19:    Plot of experimentally measured *Z´ and Z´´* vs. frequency. Data fit using a model is also shown.
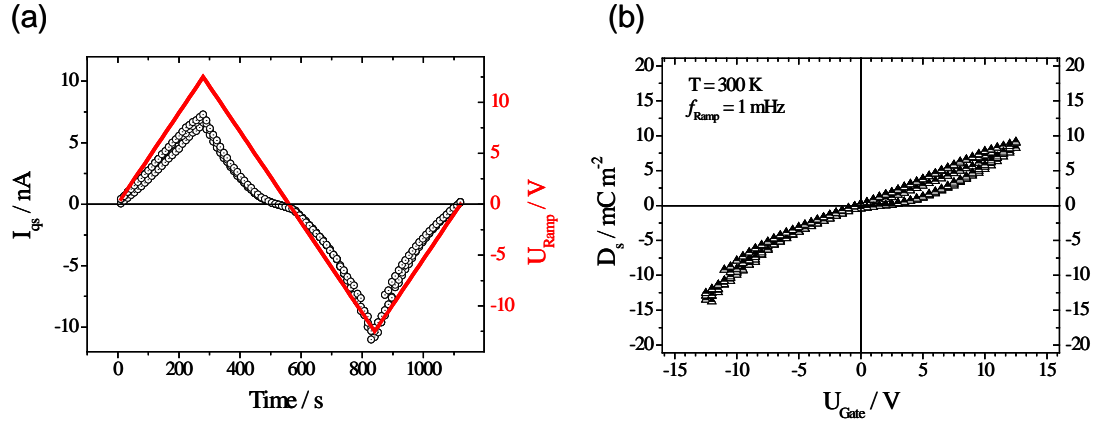


Figure 20:    Quasi-static current measured (a) as a function of an applied slow cyclic voltage ramp and (b) surface charge density as a function of a voltage ramp showing Quasi-linear charge polarisation at frequency of 1mHz.

# 5 Transient response of BiOFETs

As mentioned before, charge trapping and release time can be strong function of applied voltage as well as device temperature. Transient decay of the $I_{Drain,Sat}$ was carried out at different temperatures. As shown in Figure 21, when $I_{Drain,Sat}$ was measured at T=320 K, there exist a remnant behaviour. This remnant behaviour seems to get reduced at lower temperatures. However, there is also decrease in the magnitude of $I_{Drain,Sat}$ due to lowering of mobility of PCBM at lower temperatures. In the all the cases, at lower temperatures, it is clear that remnant $I_{Drain,Sat}$ at $V_{Gate} = 0$ V gets reduced indicating no charged species are available to give rise to remanence behaviour.
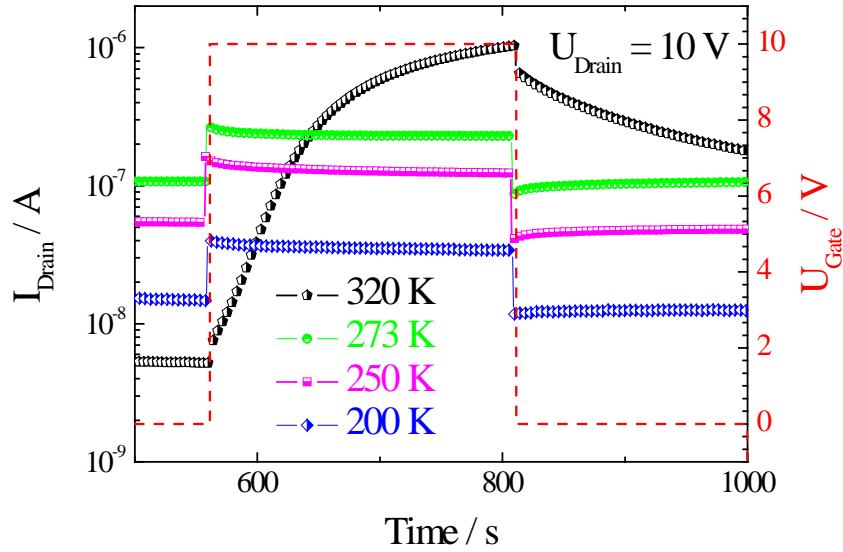


Figure 21:   Temperature dependent transient decay charactersics of $I_{Drain,Sat}$ of BioFET when a pulse of $V_{Gate}$ with pulse height as shown in right hand scale.

On the other hand, one can also get benefit by utilizing the observed remanence behaviour for use as a memory element. In Figure 22, $I_{Drain,Sat}$ is measured for a $V_{Gate}$ pulse applied for longer duration of 200s. Note the pulse voltage level is only around 20 V, thereby demonstrating that voltage levels can be reduced to values of practical interest. However, the programming time is still an obstacle to be

20

addressed in further work. After switching off the voltage pulse, the current decays, after 800 s the Ids current is still more than one order of magnitude larger than the off current. The inset of Figure 22(a) shows the retention time measurement as a function of $V_{Gate}$. $I_{Drain,Sat}$ can be depleted upon applying a depletion voltage as shown in Figure 22(b). For the measured $I_{Drain,Sat}$ one can define four states: "off", "write", "on" and "erase".
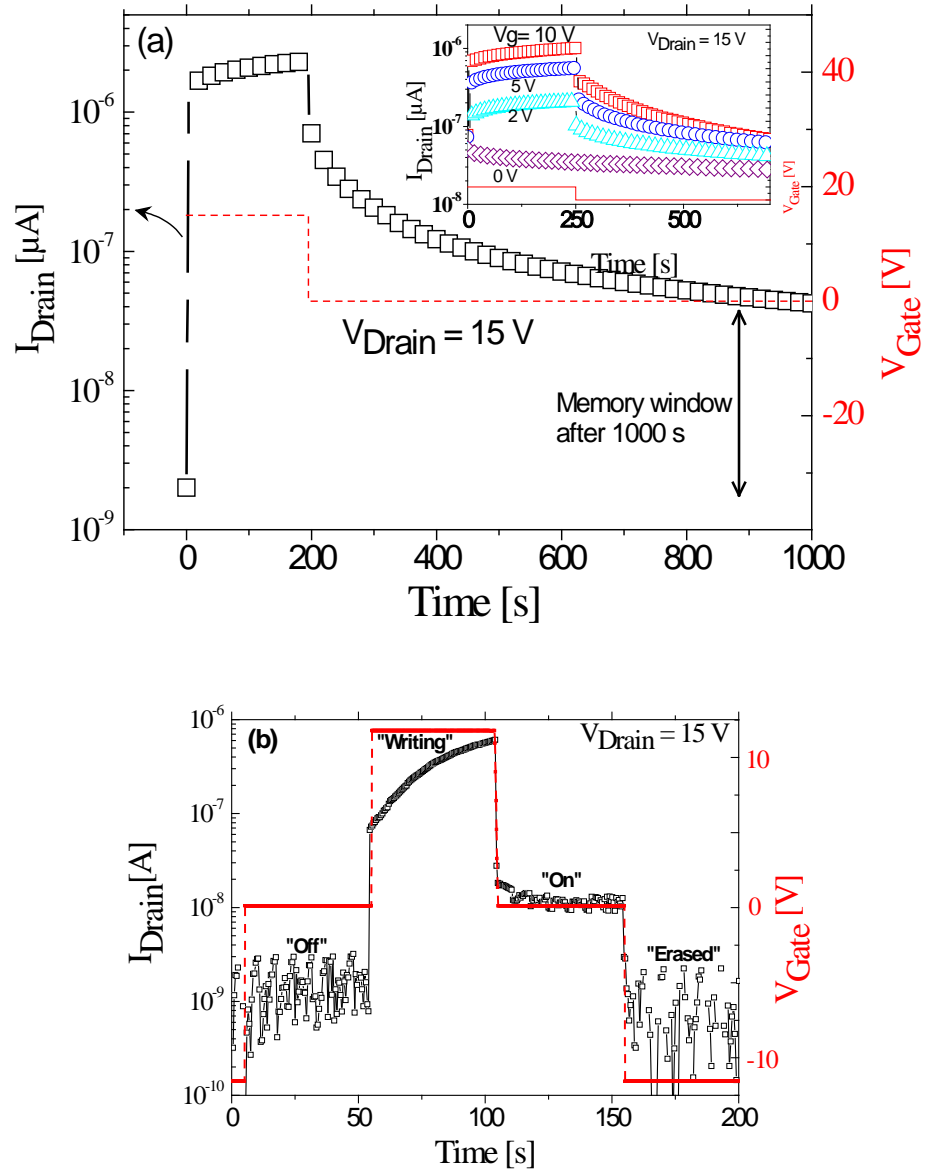


Figure 22:    Transient response characteristics of BioFETs (a) indicating a long retention time Inset: Transient decay characteristics of BioFET with different gate bias condition (b) as a memory element with an applied gate voltage pulse showing memory "off", "on", "write" and "erase". Note: Gate voltage pulse height is shown in right hand scale of each graph.

21

# 6 Getting rid of the hystheresis: New strategy of crosslinking DNA-CTMA

Above, we analyzed the observed large hystheresis in BiOFETs using DNA-CTMA complexes as a performance limiting issue. Therefore we analyzed the origin of this hystheresis and an ionic charge migration has been one of the main responsible factors for this hystheresis.[42, 43] In this section we present the idea of crosslinking the whole composite polymer for inhibiting the ion migration to improve the BiOFET transfer characteristics.[43]

A crosslinking agent, poly(phenyl isocyanate)-co-formaldehyde (PPIF), which has one crosslinking site located at every phenylene unit, is used for improving the uniformity of the crosslinking reaction between the DNA biopolymer chains and cationic surfactant complex CTMA. The resulting crosslinked DNA-CTMA films are significantly harder than the non-crosslinked films and are also resistant to the solvents used to process the films.

To prepare a crosslinked DNA-CTMA film, the DNA-CTMA is dissolved in butanol at a concentration of 0.51 M. An amount of 81.2 mol % PPIF, with respect to DNA-CTMA, is dissolved separately in butanol at a concentration of 0.51 M. Both the DNA-CTMA in butanol and PPIF in butanol solutions are mixed in a 60 $^{o}$C oven for 1 to 2 h. Once fully dissolved, the DNA-CTMA in butanol solution is added to the PPIF in butanol solution and the resulting solution is mixed for an additional 2 hours in the 60 $^{o}$C oven. The DNA-CTMA-PPIF solution is then filtered through a 0.2 µm pore size syringe filter and left to sit overnight in the 60 $^{o}$C oven. It is spin cast onto a substrate using the same spin parameters as the non-crosslinked DNA-CTMA films. The substrates are baked in an 80 $^{o}$C oven for 5 min and then cured in a vacuum oven at 175 $^{o}$C for 15 min.

First we fabricated metal-insulator-metal (MIM) and metal-insulator-semiconductor (MIS) devices for the characterization of the dielectric properties of DNA-CTMA and DNA-CTMA-PPIF films. Such films were sandwiched between a 0.6 nm/60 nm chromium/gold (Cr/Au) bottom electrode, which was evaporated on top of a quartz substrate and a 60 nm Au top electrode. An HP model 4248A instrument was used for the capacitance vs. frequency measurements. The plots of the dielectric response of the DNA-CTMA and DNA-CTMA-PPIF films (Figure 23) show that dc capacitance of DNA-CTMA-PPIF is

~0.8 nF/cm$^2$. From the measurement of capacitance per unit area, we determined a dielectric constant of $\varepsilon_{DNA/CTMA/PPIF}$= 5.4 .
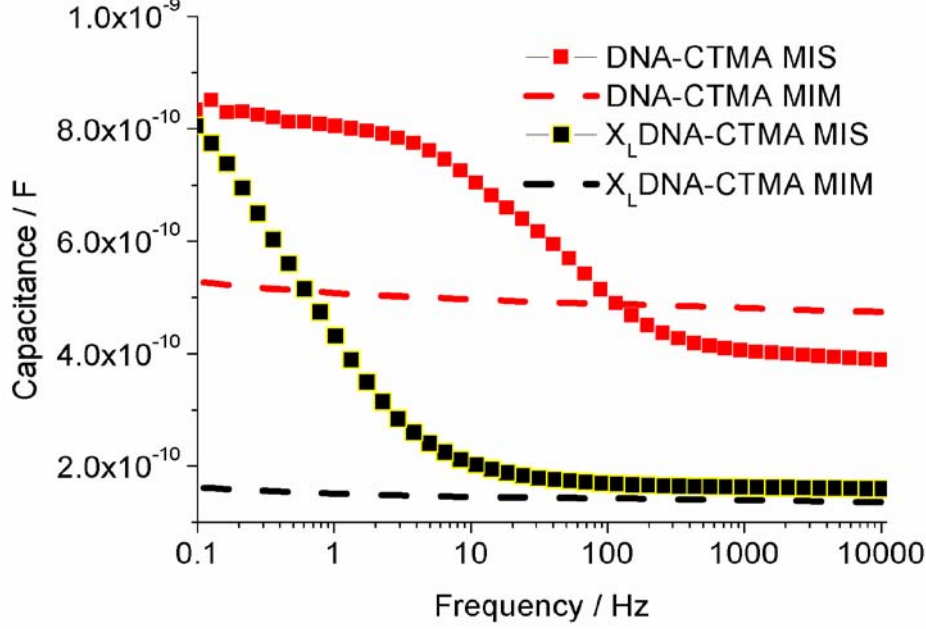


Figure 23: Room temperature capacitance-frequency characteristics of the MIM and MIS devices.

We then fabricated an n-channel BiOFET, evaporating 80 nm C$_{60}$ (Fig. 24(a)) and p-channel BiOFET evaporating 80 nm α-sexithiophene (T6) (Fig. 25(a)) as organic semiconductors. We fabricated device structures using top contact geometry on top of a layer of 0.5 µm DNA-CTMA-PPIF, serving as the gate dielectric. For two types of BiOFETs, 60 nm Au electrode was employed as the bottom contact and Cr/Au (0.6 nm/60 nm) electrodes were used as the source-drain contacts; the channel length $L$ of the device was 20 µm and the channel width was $W$ = 200 µm, giving a $W/L$ ratio of 10. All the device electrical characterization was carried out under an argon environment inside the glove box. An Agilent model E5273A with a two source-measurement unit instrument was employed for the steady state current-voltage ($I$-$V$) measurements. All measurements were performed at a scan rate of 0.2 V/s.

Figure 24(b) shows the output characteristics of n-channel BiOFET device. For an applied positive drain-source voltage $V_{ds}$ , above a positive gate voltage,

$V_{gs}$, a saturated drain current, $I_{ds}$, is observed in the range of $2 \times 10^{-7}$ A for applied $V_{gs}$ of 20 V. Transfer characteristics with applied large $V_{ds}$ of 20 V are shown in Fig. 24(c). In case of using cross-linked DNA-CTMA film as a gate dielectric, hysteresis is vanished. We also determined the linear mobilities to be $9.25 \times 10^{-3}$ and $9.34 \times 10^{-3}$ cm$^2$/V.s for n-channel BiOFET devices using crosslinked DNA-CTMA and non-crosslinked DNA-CTMA films as a gate dielectric, respectively.
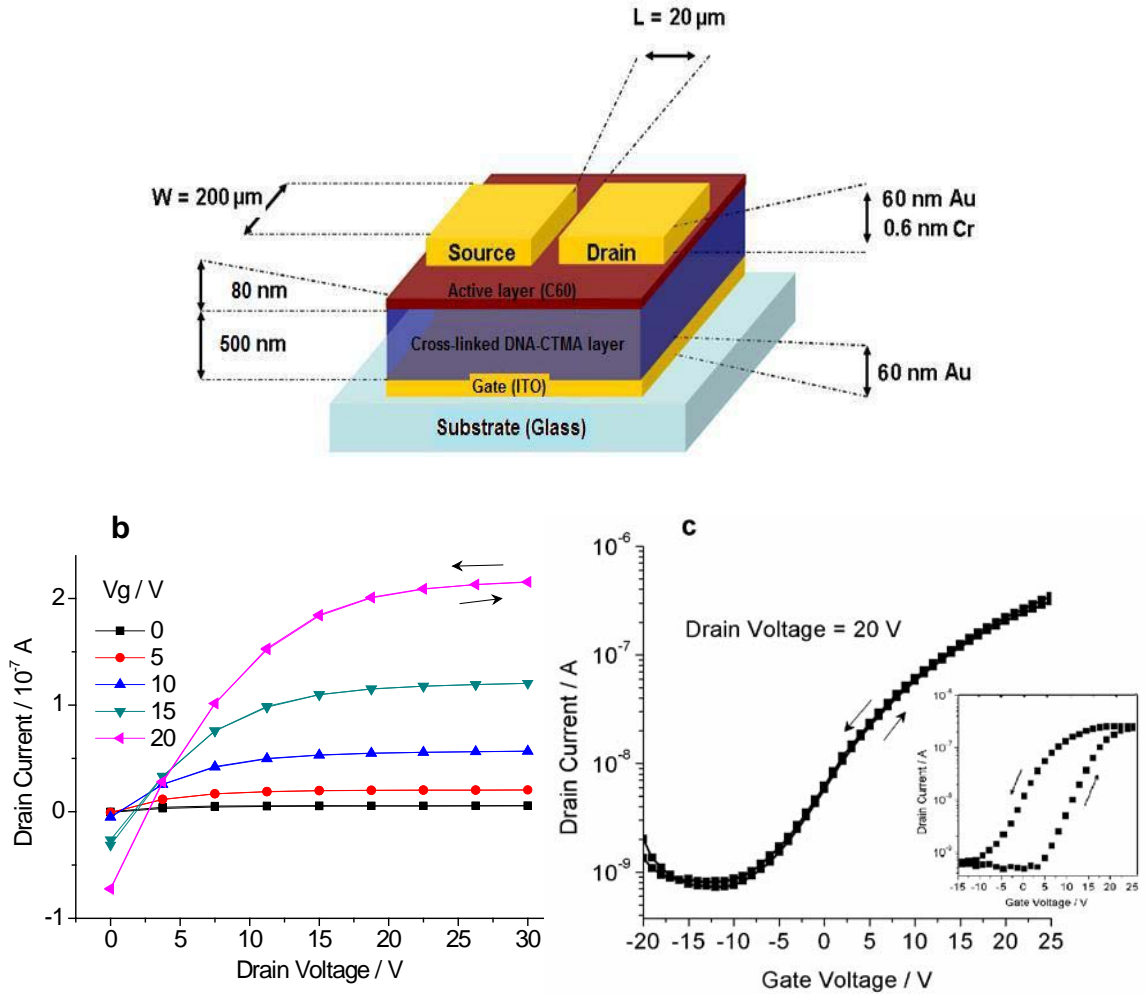


Figure 24. (a) Diagram of the n-channel BiOFET device geometry. (b) Output characteristics of BiOFET with C$_{60}$ as a semiconductor with cross-linked DNA-CTMA film as a dielectric at different gate voltages. (c) Transfer characteristics at $V_{DS} = 20$ V. Inset: Transfer characteristics of BiOFET with C$_{60}$ as a semiconductor with noncross-linked DNA-CTMA film as a dielectric as displayed in Fig. 17b above.
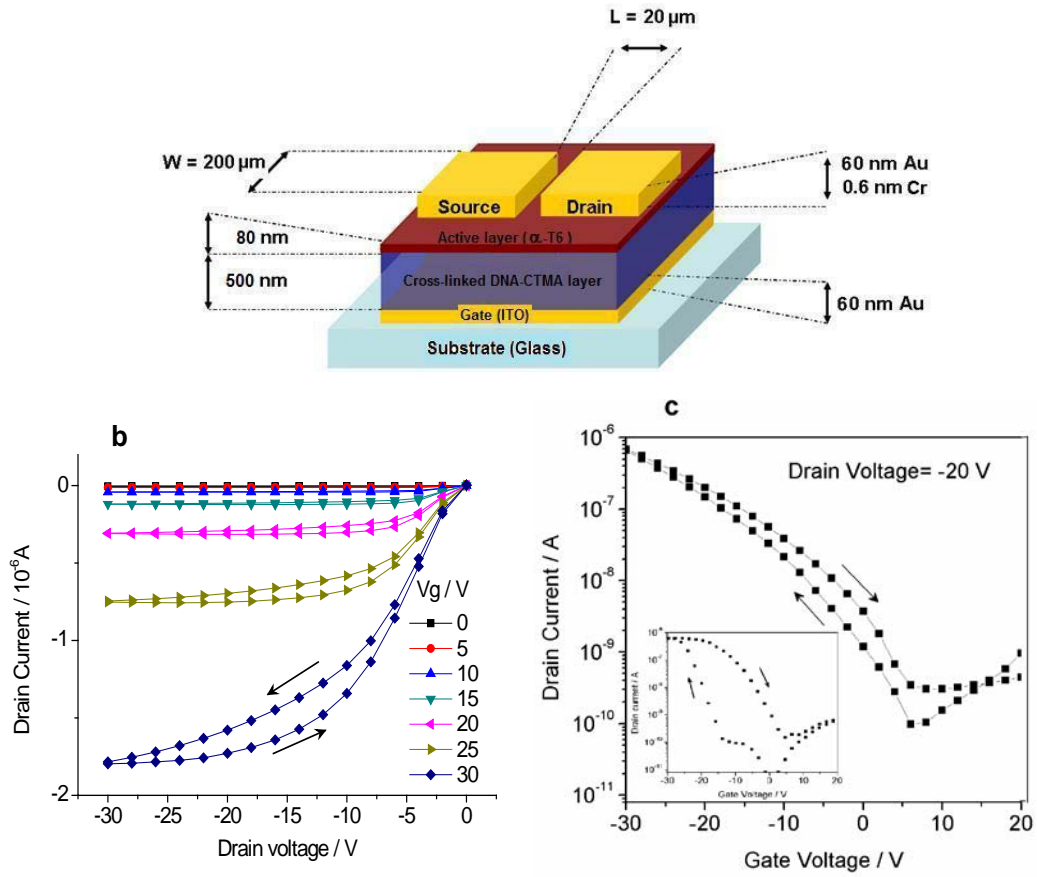
Figure 25. (a) Diagram of the p-channel BiOFET device geometry. (b) Output characteristics of BiOFET with α-T6 as a semiconductor with cross-linked DNA-CTMA film as a dielectric at different gate voltages. (c) Transfer characteristics at $V_{DS}$ = -20 V. Inset: Transfer characteristics of BiOFET with α-T6 as a semiconductor with noncross-linked DNA-CTMA film as a dielectric.

Similarly, the output characteristics and transfer curves of the p-channel BiOFET are shown in Figs. 25(b) and 25(c). The hysteresis in the transfer characteristics can also be reduced by using crosslinked DNA-CTMA dielectric. The linear mobilities are 0.42 and 0.09 $cm^2$/V.s for p-channel BiOFET devices using crosslinked DNA-CTMA and non-crosslinked DNA-CTMA films as a gate dielectric, respectively.

# 7. Summary and Outlook

Optoelectronic devices fabricated employing DNA biopolymers showed that the performance of these devices can be considerably better than their counterparts. In addition to this, biopolymers such as salmon based DNA are renewable resources and are inherently biodegradable. Additionally, molecular weight of the DNA can be tailored with the help of sonication procedure with molecular weight ranging from 200,000 to 8,000,000 Da which corresponding to 220 to 12,000 base pairs.. DNA-surfactant complexes render excellent thin films using common organic solvents. This process also enhances the mechanical properties of the resulting thin film and neutralises the charge of DNA. Large band gap, dielectric constant 7.8, fully transparent to the visible regime of the spectrum, large resistivity and thermal stability up to $230^{0}C$ make DNA-CTMA employed in various electronic devices. Although the mechanisms are not yet completely understood, it is proposed that charged species present in the bulk of DNA-CTMA and at the interface of DNA-CTMA with the organic semiconductor are likely to be responsible for the hysteresis in the transistor characteristics. We have analyzed and created a crosslinking strategy to overcome this problem.

In general the largely independent bio/lifesciences and information technologies of today can be thus bridged in an advanced cybernetic approach using organic semiconductor devices (Fig. 26). This field of bio-organic electronic devices is proposed to be the future mission of organic semiconductor devices.
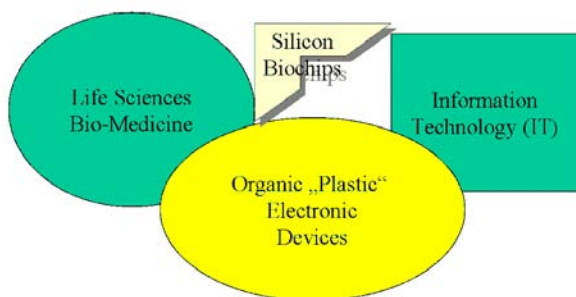


Figure 26:    Interfacing the life sciences with electronic technology (cybernetics) as future mission for organic semiconductor devices.

**References:**

[1] Huitema HE, Gelinck GH, Van Veenendaal E, Cantatore E, Touwslager FJ, et al. 2003. A flexible QVGA Display with Organic Transistors. IDW 1663

[2] G. Darlinski, U. Böttger, R. Waser, H. Klauk, M. Halik, U. Zschieschang, G. Schmid, and C. Dehm, *J. Appl. Phys*. 093708, 97 (2005).

[3] B. Crone, A. Dodabalapur, A. Gelperin, L. Torsi, H. E. Katz, A. J. Lovinger, and Z. Bao, *Appl. Phys. Lett*., 2229, 78 (2001).

[4] Robinson, B. H. & Seaman, N. C. *Protein Eng*. 1, 295–300 (1987).

[5] Yan, H., Zhang, X., Shen, Z. & Seeman, N. E. *Nature* 415, 62–65 (2002).

[6] Turberfield, A. *Phys. World* 16, 43 (March 2003).

[7] E. Braun, Y. Eichen, U. Sivan, G. B. Yoseph*, Nature*, 775, 291 (1998).

[8] P. J. de Pablo, F. Moreno-Herrero, J. Colchero,J. Gómez Herrero,P. Herrero,A. M. Baró, Pablo Ordejón,José M. Soler, and Emilio Artacho, *Phys. Rev. Lett.*, 4992, 85 (2000).

[9] L. Cai, H. Tabata and T. Kawai, *Appl. Phys. Lett*. 3105, 77 (2000).

[10] A. J. Storm, J. van Noort, S. De Vries, and C. Dekker, *Appl. Phys. Lett*. 3881, 79 (2001)

[11] J. S. Hwang, K. J. Kong, D. Ahn, G. S. Lee, D. J. Ahn, S. W. Hwang, *Appl. Phys. Lett.* 1134, 81 (2002).

[12] Y. Zhang, R. H. Austin, J. Kraeft, E.C. Cox,and N. P. Ong, *Phys. Rev. Lett*., 198102, 89 (2002).

[13] D. Porah, A. Bezrydin, S. de Vries, C. Dekker, *Nature*, 635 , 403 (2000).

[14] Y. Yang, P. Yin, X. Li, and Y. Yan, *Appl. Phys. Lett*. 203901 (2005)

[15] H. Fink and C. Schönenberger, *Nature* 407, 398 (1999).

[16] A. Yu. Kasumov, M. Kociak, S. Guéron, B. Reulet, V. T. Volkov, D. V. Klinov and H. Bouchiat, *Science,* 291, vol. 280 No. 5502 (2001).

[17] L. Wang, J. Yoshida, N. Ogata, S. Sasaki, and T. Kajiyama, *Chemistry of Materials*, 13(4), 1273 (2001).

[18] G. Zhang, L. Wang, J. Yoshida and N. Ogata, *SPIE Proc. – Optoelectronic, Materials and Devices for Communications*, eds., Q. Wang and T. Lee, 4580, 337 (2001).

[19] R. Ghirlando, E. J. Wachtel, T. Arad; A. Minsky, *Biochem*. 7110, 31 (**1992)**.

[20] K. Tanaka, Y. Okahata, *J. Am. Chem. Soc.,* 1996, 118, 10679

[21] H. Kimura, S. Machida, K. Horie, Y. Okahata, *Polymer Journal*, 1998, 30, 708

[22] J. Grote, N. Ogata, J. Hagen, E. Heckman, M Curley, P. Yaney, M. Stone, D. Diggs, R. Nelson, J. Zetts, F. Hopkins and L. Dalton, *SPIE Proc. – Nonlinear Optical Transmission and Multiphoton Processes in Organics*, eds., A. Yates, K. Belfield, F. Kajzar and C. Lawson, 5221, 53, (2003)

[23] Emily M. Heckman, Perry P. Yaney, James G. Grote, F.Kenneth Hopkins, Melanie M. Tomczak, *Proceedings of SPIE – 6117*, 61170K, 2006

[24] Emily M. Heckman, Joshua A. Hagen, Perry P. Yaney, James G. Grote, F. Kenneth Hopkins, *Applied Physics Letters*, 87,211115, 2005.

[25] Grote, J. G. *et al*. *Proc. SPIE* 5934, 593406 (2005).

[26] Subramaniam, G., Heckman, E., Grote, J. & Hopkins, F. *IEEE Microwave Wireless Comp. Lett.* 15, 232–234 (2005).

[27] Joshua A. Hagen, Weixin X. Li, James G. Grote, and Andrew J. Steckl, *Applied Physics Letters*, 88, 171109, 2006.

[28] For a review article on OFET : Th. B. Singh and N. S. Sariciftci, *Annual Review of Material Research 36*, 199 (2006).

[29] H. Klauk, M. Halik, U. Zschieschang, G: Schmid, W. Radlik, *J. App. Phys.* 92, 5259 (2002)

[30] R. Parashkov, E. Becker, G. Ginev, T. Riedl, H. H. Johannes, and W. Kowalsky, *J. Appl. Phys.* 95, 1594 (2006).

[31] J. Park, S. Y. Park, S. Shim, H. Kang and H. H. Lee, *Appl. Phys. Lett.* 85, 3283 (2004).

[32] R. Schroeder, L. A. Majewski and M. Grell, *Appl. Phys. Lett.* 83, 3201 (2003)

[33] D. Knipp, R. A. Street, B. Krusor, J. Ho, R. B. Apte, *Mat. Res. Soc. Symp. Proc.* 708 ,BB.10 (2002).

[34] R. Schroeder, L. A. Majewski and M. Grell, *Adv. Mater.* 16, 633 (2004)

[35] Th. B. Singh, N. Marjanović, G. J. Matt, N. S. Sariciftci, R. Schwödiauer and S. Bauer,. *Appl. Phys. Lett.* 85, 5409 (2004)

[36] R. C. G. Naber, C. Tanase, P. W. M. Blom, G. H. Gelinck, A. W. Marsman, F. J. Touwslager, S. Setayesh and D. M. De Leeuw *Nature Mater.* 4, 243 (2005).

[37] Th. B. Singh, N. Marjanović, P. Stadler, M. Auinger, G. J. Matt, S. Günes, N. S. Sariciftci, R. Schwödiauer and S. Bauer, *J. Appl. Phys.* 97, 083714 (2005).

[38] Th. B. Singh, N.S. Sariciftci, J. Grote, F. Hopkins, *Journal of Applied Physics* 100 (2006), 024514.

[39] P. Stadler, K. Oppelt, B. Singh, J. Grote, R. Schwödiauer, S. Bauer, H. Piglmayer-Brezina, D. Bäuerle, N.S. Sariciftci, *Organic Electronics* 8 (2007), 648-654.

[40] P. Stadler, Master thesis, Linz Institute of Organic Solar Cells (LIOS), Johannes Kepler University of Linz, Austria, 2007

[41] F. Kremmer and A. Schönhals eds.; *Broadband Dielectric Spectroscopy*,

Spinger-Verlag Berlin Heidelberg 2003. pp. 87.

[42] M. Egginger, M. Irimia-Vladu, R. Schwödiauer, A. Tanda, I. Frischauf, S. Bauer, N.S. Sariciftci, *Adv. Mat*. 20, 1018 (2008).

[43] C. Yumusak, B. Singh, N.S. Sariciftci, G. Grote, *Applied Physics Letters* 95 (2009), 263304